SAND2014-20040C

Semi-Supervised Classification of Terrain Features in Polarimetric SAR Images using $H/A/\bar{\alpha}$ and the General Four-Component Scattering Power Decompositions

Stephen Dauphin*†, R. Derek West†, Robert Riley†, and Katherine M. Simonson†

*Mathematics Department, Colorado State University, Fort Collins, Colorado 80523-1874
†Sandia National Laboratory, Albuquerque, New Mexico, 87123
SAND2014-*To Be Entered Later*

***Abstract*—In an effort to enhance image classification of terrain features in fully polarimetric SAR images, this paper explores the utility of combining the results of two state-of-the-art decompositions along with a semi-supervised classification algorithm to classify each pixel in an image. Each pixel is labeled either with a pre-determined classification label, or labeled as unknown.**

I. Introduction

In this paper, we introduce a novel semi-supervised terrain classification framework for polarimetric SAR imagery. The training consists of selecting small regions of homogeneous terrain for each terrain category of interest from a training image. Probabilistic models are generated from these homogeneous regions . In the test image each pixel in the image (or stack of images) is labeled with one of the training categories. The proposed classification approach uses eight parameters from two well-known polarimetric decompositions which describe the physical nature of the scatterers within each pixel. The probabilistic modeling, which occurs during training, fits probability density functions (pdfs) to each of the eight parameters for each region. The eight parameters of every pixel in the test images are each compared with the corresponding pdf, and assigned a p-value. The eight p-values for each pixel are fused together to give each pixel a probability value for fitting each terrain region. This probability determines the terrain region label it is assigned to. If the probability is below a set threshold (which corresponds directly to the desired probability of detection), the pixel is labeled unclassified.

II. PolSAR Background

A. Brief Overview of Polarimetric SAR

A Polarimetric SAR (PolSAR) system measures the polarimetric information of the back scatter from the reflectors in a scene. The measured data are formed into four complex-valued images, HH, HV, VH, VV, where HV represents the intensity of a vertically polarized return of an emitted horizontally polarized signal. These four polarization states form a basis for all polarization states and therefore contain the complete polarization information of the backscatter. Through the use of polarimetric decompositions, we can extract physically meaningful properties of the scatterers contained in each pixel of the image based on the intensity and the polarization of the response.

B. PolSAR decompositions

Two of the widely used building blocks of many polarimetric decompositions are the Pauli feature vector, $\underline{\boldsymbol{k}}$, and the corresponding coherency matrix, $\boldsymbol{T}$ [1]. For the monostatic case, $\underline{\boldsymbol{k}}$ is a three element vector

$$\underline{\boldsymbol{k}} = \frac{1}{\sqrt{2}} \begin{bmatrix} HH + VV \\ HH - VV \\ 2HV \end{bmatrix} \tag{1}$$

and $\boldsymbol{T}$ is a 3×3 matrix denoted by $\boldsymbol{T}_3$.

$$\langle \boldsymbol{T}_3 \rangle = \left\langle \underline{\boldsymbol{k}} \cdot \underline{\boldsymbol{k}}^{*\mathrm{T}} \right\rangle \tag{2}$$

Both quantities are built from the four complex images where $\langle \cdot \rangle$ is a spatial ensemble average and $\underline{\boldsymbol{k}}^{*\mathrm{T}}$ the conjugate transpose of $\underline{\boldsymbol{k}}$.

Several classes of polarimetric decompositions exist to extract physically meaningful characteristics of the scatterers. In the proposed classification approach a model-based decomposition and an eigenvalue decomposition are used.

$G4U$ is a model-based decomposition that divides the total power response of each pixel into cannonical scatter types [2]. The $G4U$ decomposition is an extension of Yamaguchi's four-component decomposition [3] which is built upon Freeman/Durden's novel three component decomposition [4]. The $G4U$ separates the total power into independent scattering mechanisms: odd-bounce power (also refered to as surface power) $\boldsymbol{P_s}$, even-bounce power (also refered to as dihedral or double-bounce power) $\boldsymbol{P_d}$, volumetric power $\boldsymbol{P_v}$, and helical power $\boldsymbol{P_c}$. The coherency matrix for each pixel is separated into the theoretical coherency matrices for these four

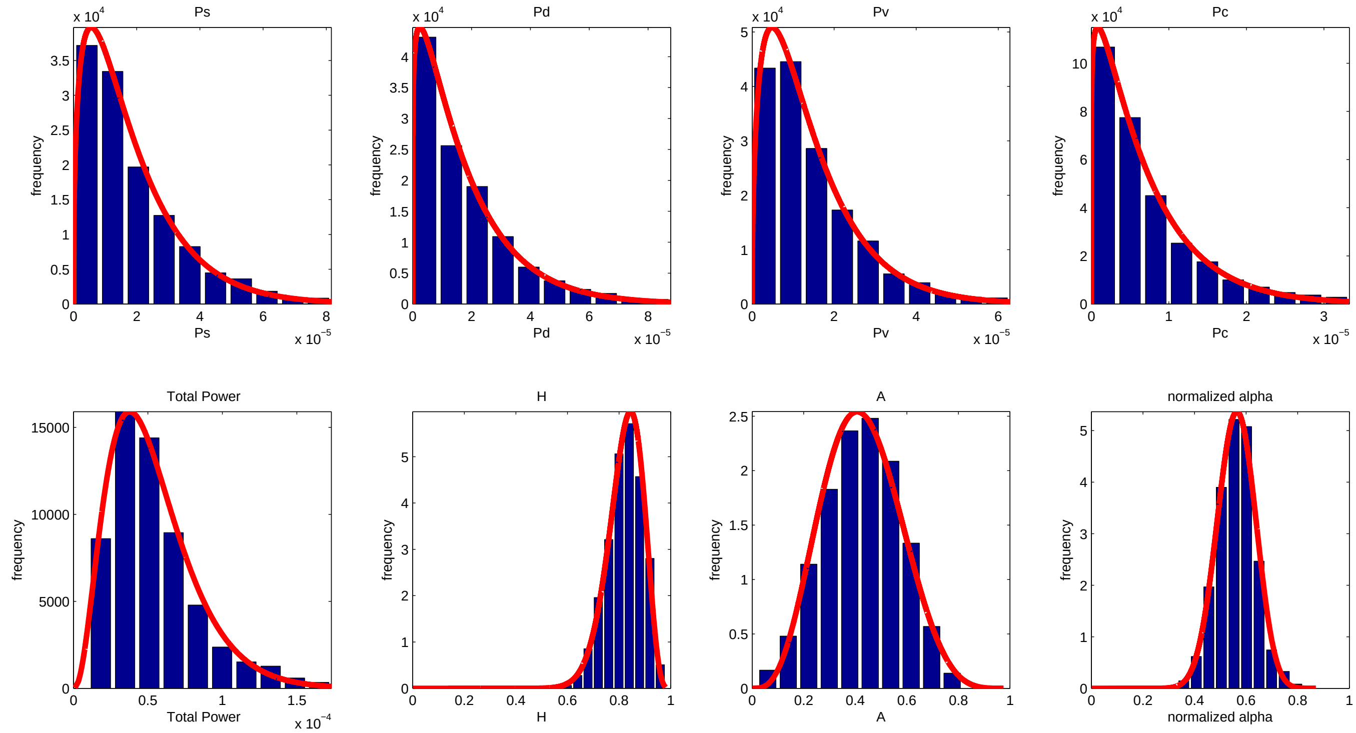

Fig. 1: Historgrams of the eight parameters of selected pixels for one category
The red plot represents the distribution that is fit to the data

scattering mechanisms with power coefficients and the $G4U$ decomposition solves for these coefficients.

$$\langle[T_3]\rangle = P_s \langle[T_3]\rangle_{surface} + P_d \langle[T_3]\rangle_{double} \quad (3)$$

$$+P_v \langle[T_3]\rangle_{volume} + P_c \langle[T_3]\rangle_{helical} \quad (4)$$

$H/A/\bar{\alpha}$ is an eigenvalue-based decomposition [5] which uses the eigenvalues and eigenvectors of the coherency matrix, $\boldsymbol{T}_3$, to compute polarimetric parameters. The eigenvalues are used to create psuedoprobabilities. These psuedoprobabilities are used to calculate a average roll-invariant parameter ($\bar{\boldsymbol{\alpha}}$) and an entropy parameter ($\boldsymbol{H}$). An anisotropy parameter, ($\boldsymbol{A}$), is calculated with the smaller two eigenvalues of the coherency matrix.

These two fundamentally different decompositions were chosen in an effort to combine the added benefits of the additional information of the model-based $G4U$ scatter type powers with the statistical $H/A/\bar{\alpha}$ parameters soley determined by the coherency matrix.

III. Proposed Approach

The two decompositions, $G4U$ and $H/A/\bar{\alpha}$, are run on the set of complex-valued images. From the results of these decompositions, each pixel has the following eight parameters associated with it: $\boldsymbol{P_s}, \boldsymbol{P_d}, \boldsymbol{P_v}, \boldsymbol{P_c}, \boldsymbol{H}, \boldsymbol{A}, \bar{\boldsymbol{\alpha}}$ values along with total power $\boldsymbol{TP}$. At this point, the SLIC superpixel segmentation algorithm [6] is used as a method to quickly and easily select homogeneous (or *nearly* homogeneous) pixels of interest for training. Each parameter of the selected pixels (representing a desired category) are fit to parametric probability density functions using method of moments parameter estimation. For the proposed approach, Gamma distributions are fit to the parameters $\boldsymbol{P_s}, \boldsymbol{P_d}, \boldsymbol{P_v}, \boldsymbol{P_c}$, and $\boldsymbol{TP}$. Beta distributions are fit to the parameters $\boldsymbol{H}$, $\boldsymbol{A}$, and $\bar{\boldsymbol{\alpha}}$ (normalized). Every parameter of every pixel in the image is given a p-value corresponding to how well the parameter fits the modeled distributions from the training data categories. Thus, every pixel in the image has eight p-values.

A probabilistic fusion framework [7] is used to combine the p-value scores into one value that represents the probability that the pixel belongs to the distributions of the selected pixels and therefore belongs to the class the selected pixels represent. Let F_i be the pdf of the i^{th} characteristic, and let $P_i(x)$ be the probability that the i^{th} parameter of a pixel fits the distribution. As long as F_i is continuous (or well approximated by a continuous function), then the random variable P_i of the selected pixels has a distribution that is uniform on $[0, 1]$. The P_i of pixels that do not belong to the distribution will not be uniform.

Let $Y_i = -\log(P_i)$. The log of a uniform distribution is the standard exponential. Y_i will be very large for pixels with at least one characteristic that has low probability of fitting the distribution of the selected pixels.

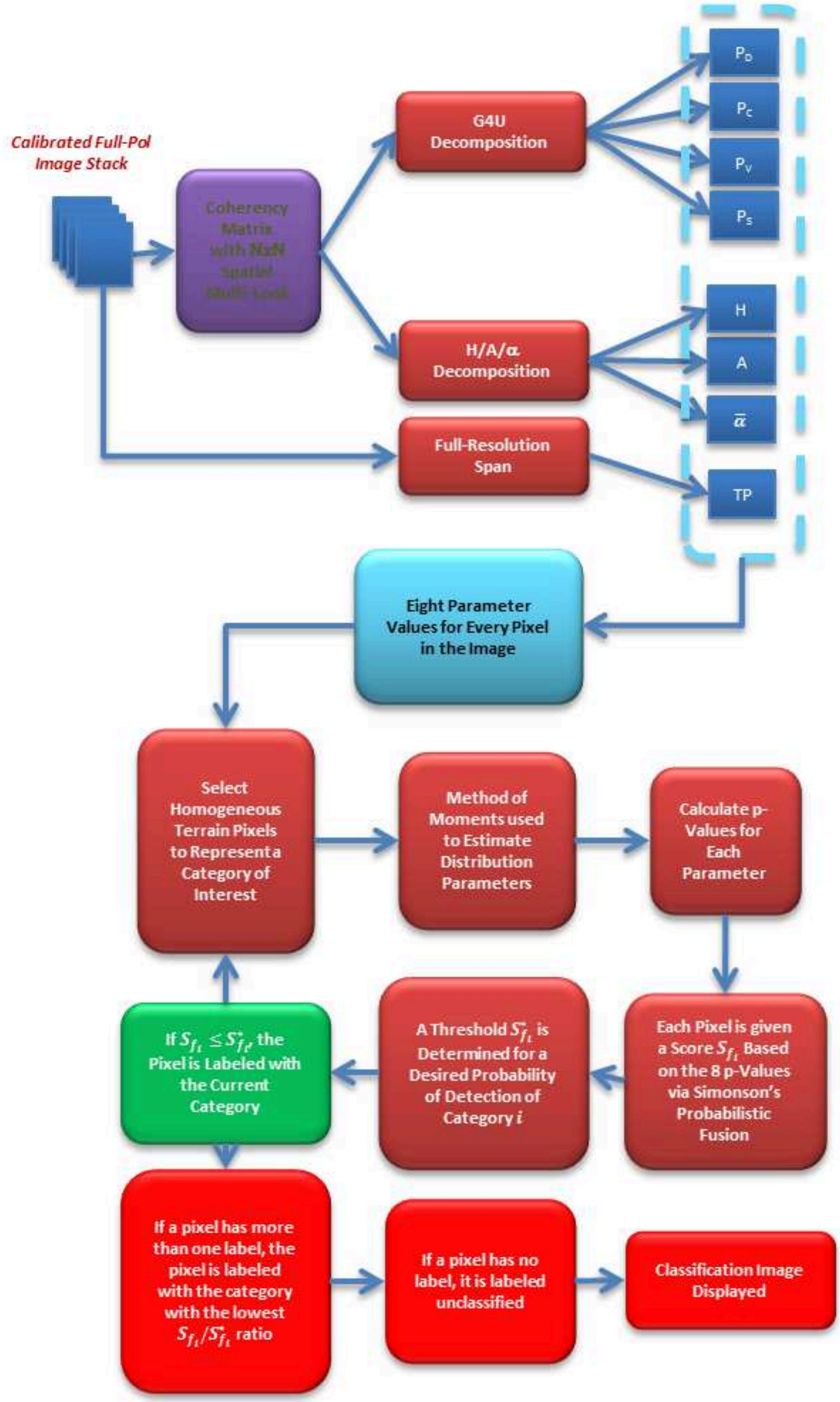

Fig. 2: Flow chart illustrating the proposed classification method

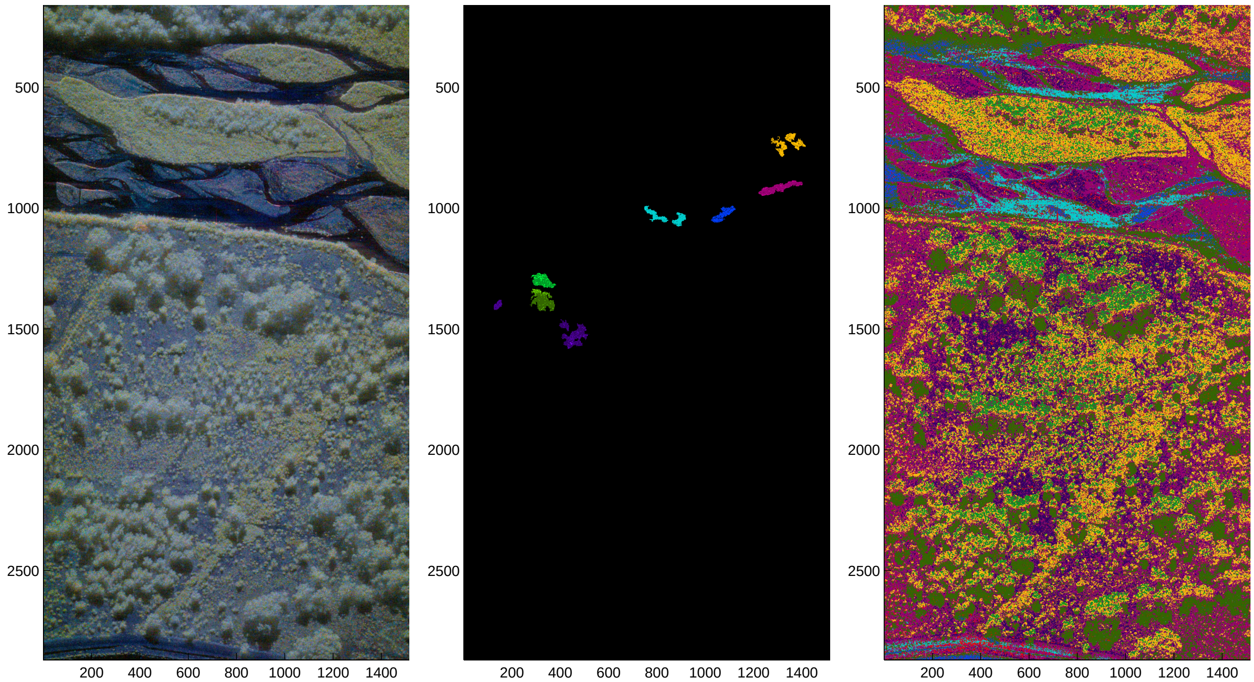

(a) G4U image: with $\boldsymbol{P_s}$ blue, $\boldsymbol{P_d}$ red, $\boldsymbol{P_v}$ green, $\boldsymbol{P_c}$ yellow

(b) Hand-selected pixels of each homogeneous region

(c) Pixel by pixel classification result corresponding to the categories selected in 3b

Fig. 3: Results

Legend	
Ground Vegetation	
Vegetation Shadow	
Tree Tops	
Shallow Water	
Deeper Water	
Hard-packed Dirt	
Sand/Loose Dirt	
Unclassified	

Let

$$S_f = \sum_{i=1}^{N} Y_i \tag{5}$$

where N represents the number of characteristics to combine. For the example in this paper, $N = 8$. The sum of N independent standard exponentials is represented by a gamma distribution with $r = N$ and $\lambda = 1$. Therefore, if the Y_i values are independent, the sum is represented with a gamma distribution with the theoretical parameters ststed above. If the Y_i values are not independent, as with the parameters used in the proposed approach, their sum is still gamma distributed, but the parameters need to be computed with the correlation taken into account. Let $\hat{\rho}_{ij}$ be the estimated correlation between Y_i and Y_j. Then

$$C = \sum_{i=1}^{N} \sum_{j \neq i} \hat{\rho}_{ij} \tag{6}$$

is the correlation correction factor that can be used to account for correlations bewteen the parameters. Accounting for correlation, the distribution of S_f is gamma distributed with parameters:

$$\hat{r} = \frac{N^2}{N+C} \qquad \hat{\lambda} = \frac{N}{N+C} \tag{7}$$

A threshold S_f^* can be selected so that the probability that a gamma random variable with the above parameters in Equation (7) is less than S_f^*, matches the desired probability of detection. A pixel is labeled with a category if the pixel's S_f parameter is less than or equal to the category's S_f^* threshold; otherwise, the pixel remains unclassified. If a pixel is labeled with two or more categories, the pixel is labeled with the category that yields the lowest $\frac{S_f}{S_f^*}$ ratio. The proposed classification is illustrated with the flow chart in Figure 2.

IV. Experimetal Results

The data for this example were collected along the Rio Grande River in Albuquerque, New Mexico, with the Sandia National Laboratories fully-polarimetric X-band development radar.

The histograms shown in figure 1 are of the eight parameters of the hand-selected pixels for the category of vegetation shadow. Overlayed on the histograms are the estimated distributions computed using the method of moments parameter estimation from the hand-selected pixels. The eight parameters of each pixel in the image are compared to these distributions and are each given a p-value representing the probability that the pixel's parameters fit the corresponding distributions of the category's hand-selected pixels.

The three images shown in figure 3 are the $G4U$-colored PolSAR image 3(a), the hand-selected pixels representing the categories are represented in image 3(b), and the classification result in image 3(c). The $G4U$ is a false-color PolSAR image with the color representing each pixel's scattering mechanism contributions represented by the percetage of $\boldsymbol{P_s}$ blue, $\boldsymbol{P_d}$ red, $\boldsymbol{P_v}$ green, $\boldsymbol{P_c}$ yellow, and the power of the return represented by pixel brightness. Image 3(b) illustrates the hand-selected pixels that generate the categories. The number of pixels selected per category has an order of magnitude of 10^2 compared to the number of pixels in the image 4.5×10^6. The different colors represent different categories. The legend for the colors of the categories is shown in table III. Image 3(c) is the resulting pixel-by-pixel classified image.

V. Conclusion

We have proposed semi-supervised terrain classification framework, which classifies each pixel into classes defined by the hand-selected homogeneous training regions. If the pixel is not a close match to any of homogeneous terrain regions, it is flagged as uncategorized.

References

[1] J. Lee and E. Pottier, *Polarimetric Radar Imaging: From Basics to Applications*. CRC Press, 2002.

[2] G. Singh, Y. Yamaguchi, and S.-E. Park, "General four-component scattering power decomposition with unitary transformation of coherency matrix," *Geoscience and Remote Sensing, IEEE Transactions on*, vol. 51, no. 5, pp. 3014–3022, May 2013.

[3] Y. Yamaguchi, T. Moriyama, M. Ishido, and H. Yamada, "Four-component scattering model for polarimetric SAR image decomposition," *Geoscience and Remote Sensing, IEEE Transactions on*, vol. 43, no. 8, pp. 1699–1706, 2005.

[4] A. Freeman and S. Durden, "A three-component scattering model for polarimetric SAR data," *Geoscience and Remote Sensing, IEEE Transactions on*, vol. 36, no. 3, pp. 963–973, May 1998.

[5] S. Cloude and E. Pottier, "An entropy based classification scheme for land applications of polarimetric SAR," *Geoscience and Remote Sensing, IEEE Transactions on*, vol. 35, no. 1, pp. 68–78, 1997.

[6] R. Achanta, A. Shaji, K. Smith, A. Lucchi, P. Fua, and S. Süsstrunk, "SLIC superpixels compared to state-of-the-art superpixel methods," *Pattern Analysis and Machine Intelligence, IEEE Transactions on*, vol. 34, no. 11, pp. 2274–2282, Nov 2012.

[7] K. M. Simonson, "Probabilistic fusion of ATR results," Sandia National Laboratories, Albuquerque, New Mexico 87185 and Livermore, California 94550, Technical report SAND98-1699, August 1998.